Performance of Several Present Weather Sensors as Precipitation Gauges

Kai C. Wong
Meteorological Service of Canada, 4905 Dufferin Street, Toronto, Ontario, Canada
Phone: (416) 739-4139, Fax: (416) 739-5721, kai.wong@ec.gc.ca

Abstract

In addition to determining the types of weather, a present weather sensor also reports on the precipitation amount and rate, thus it can function as a precipitation gauge. In this work, the performance of several present weather sensors operating as precipitation gauges is studied. The present weather sensors included in this study are OTT Parsivel, Vaisala PWD22 and Qualimetrics/AWI POSS (Precipitation Occurrence Sensor System). The precipitation accumulations reported by these present weather sensors are compared to that of a number "traditional" precipitation gauges, with a Geonor gauge in a World Meteorological Organization (WMO) double fence serving as a reference. To gain a broader perspective, the comparison is carried out under various conditions such as different precipitation types and intensities. It is hoped that the results will help to shed light on the question of whether a present weather sensor can be a viable replacement of a traditional precipitation gauge.

1 Introduction

A present weather sensor (PWS) estimates a certain aspect of the weather (i.e., qualitative descriptions of phenomena observed in the atmosphere or on the Earth's surface) at the time of observation on the basis of physical measurements. Generally a PWS determines whether precipitation occurs at the site, and if it does, the type of precipitation such as drizzle, rain or snow. Some of PWS also determines whether atmospheric obscuration (e.g. fog) exists. This determination of weather is achieved using a number of methods and technologies, but all in some way involving the estimation of the precipitation intensity. As a result, a PWS generally provides, in addition to the type of precipitation, estimations on the precipitation rate and amount. The focus of this work is the performance of the precipitation amount estimation.

This paper describes the performance of precipitation amount measurements of OTT Parsivel, Vaisala PWD22 and Qualimetrics/AWI POSS, installed at the Observing Systems and Engineering (OS&E) test site at the Centre for Atmospheric Research Experiment (CARE) at Egbert, Ontario, Canada, for the period from November 10, 2008 to June 30, 2009. The accumulations of these PWSs are compared to that of a number of weighing precipitation gauges, under various conditions such as different precipitation types and wind conditions. The weighing precipitation gauges included in the study are a Vaiasla VRG101, two Pluvio[1] and two Pluvio[2] gauges, and three Geonor gauges with one of them installed in a WMO double fence serving as a reference. This work continues the effort in [20].

2 Previous Studies

There are two previous studies ([5] and [14]) on the use of present weather sensors as precipitation gauges. In [5] the ability of the Laser Precipitation Monitor (LPM) in measuring rainfall amount and intensity is assessed. The LPM is a present weather sensor based on an optical laser disdrometer, which measures the size and vertical velocity of the hydrometers falling through a 1 mm thick laser light sheet. The size of the measurement area is approximately 46 cm^2. The daily rainfall amount measured by the LPM is compared with that of a pit gauge. All three LPMs in the test measure significantly higher rainfall amount than the pit gauge, with mean deviation ranging from + 5.3% to +20.2%. The rain intensity from the LPMs is compared to the rate calculated from the raw measurement of an OTT Pluvio precipitation gauge, using an algorithm developed by the authors. The intensity measured by the LPMs ranges from +19.2% to +37.2% higher than that of the reference. The LPM has a tendency to overshoot at the intensity peak.

In [14] the Precipitation Occurrence Sensor System (POSS) is evaluated as a gauge for measuring rain and snow amounts. POSS is a bistatic, continuous wave, X-band radar. The rate is integrated over a period of 6 hours or more, and the accumulated amount is then compared to a reference amount. The pit gauge or type B rain gauge is used as a reference for liquid and the Double Fence Intercomparison Reference (DFIR) or Nipher snow gauge is used as a reference for snow. For liquid precipitation the median of the catch ratio distribution is 82% and the interquartile range (IQR) is -12% to +19% about the median when the pit gauge is used as the reference. For solid precipitation the median of the catch ratio distribution is 90% and the IQR is -17% to +24% about the median when DFIR is used as the reference.

3 Test Site

The PWSs and weighing gauges were installed at the OS&E test site at Egbert, Ontario. The site is located 80 km north of Toronto in a rural agricultural and forested region. The latitude, longitude and elevation are 44°13'58.44"N, 79°46'53.28"W and 249 m respectively. A Google image of the test site is shown in Figure 1. The measurements of a RM Young wind sensor at 2 metres and of a temperature sensor in Stevenson screen are also used for the analysis. The locations of the sensors used in this study are also shown in Figure 1.

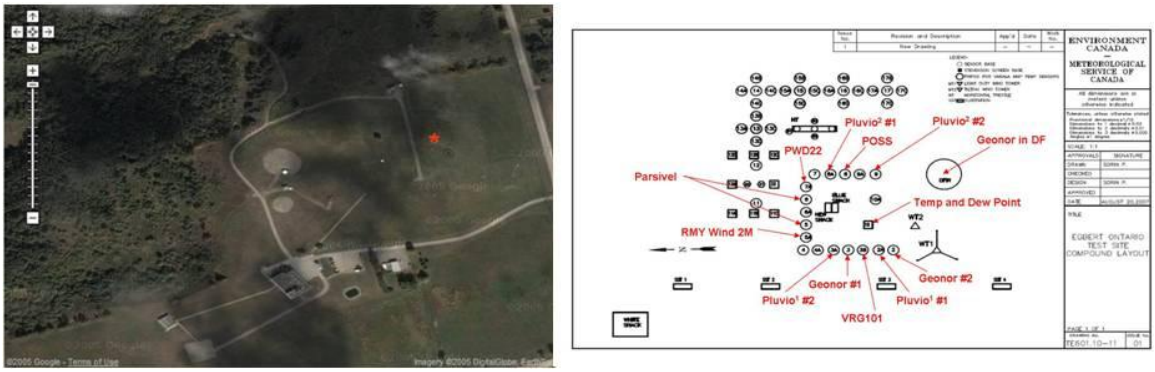

Figure 1 – CARE site with the OS&E test site indicated by the star and the layout.

4 Sensors

4.1 OTT Parsivel

OTT Parsivel is a laser-based optical disdrometer (Figure 2 (a)) for simultaneously measuring the size and velocity of all types of hydrometeors during precipitation ([7] and [6]). The transmitter generates a 1 mm thick, horizontal light sheet of 30 mm in width and 180 mm in length, resulting in a measurement area of 54 cm^2. The sensor determines the size and velocity of a hydrometeor by measuring the light extinction caused by the hydrometeor falling through the light sheet. The amount of this reduction in light is used to estimate the size of the particle, and the fall velocity of the particle is derived from the duration of the reduction. The hydrometeor is then classified into 32 classes of sizes and velocity. From the size and velocity distribution information over the measurement period, the precipitation type, rate and amount are determined.

At Egbert, there are two Parsivel sensors, referred to as Par #1 and Par #2, and both of them were mounted on posts about 3 m above the field surface.

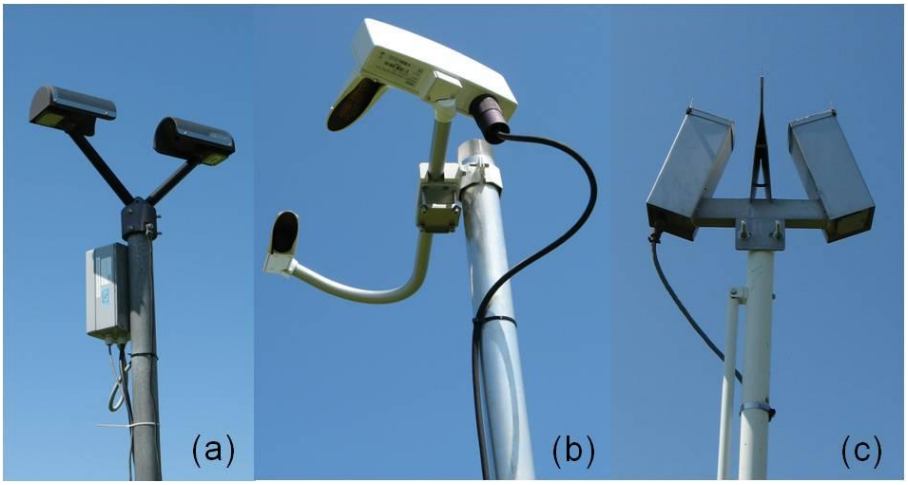

Figure 2 – OTT Parsivel present weather sensor (a), Vaisala PWD22 present weather detector (b), Qualimetrics/AWI POSS (C).

4.2 Vaisala PWD22

Vaisala Present Weather Detector PWD22 (Figure 2 (b)) is an optical sensor that measures visibility, precipitation intensity, and precipitation type [18]. The visibility is determined by measuring the forward optical scattering by the particles in the measurement volume which is about 100 cm^3. The sensor calculates the precipitation intensity by analyzing the rapid signal changes caused by the precipitation droplets. This intensity estimate is proportional to the volume of the precipitation droplets. For precipitation type identification, PWD22 also estimates the water content of the precipitation using a rain sensor. The intensity obtained from the optical measurement and the intensity from the rain sensor measurement together with an air temperature measurement allow for the identification of precipitation types. The precipitation intensity reported by the sensor is calculated from both optical and rain sensor intensity estimates.

The PWD22 was mounted on a post 3 m above the ground.

4.3 Qualimetrics/AWI POSS

The POSS (Figure 2 (C)) is a bistatic, continuous wave, X-band Doppler radar [13]. The transmitter and receiver are angled from the vertical by 20° and are mounted 45 cm apart, and their antenna axes intersect at about 34 cm above the radome windows. The transmitter continuously radiates at 10.525 GHz (2.85 cm wavelength) at a nominal output power of 100 mW. POSS measures the Doppler signals of hydrometeor falling through its sampling volume (of the order of a cubic meter depending on the hydrometeor size) which extends up to about 2 m above the sensor. From these signals, a Doppler power density spectrum is computed and the occurrence, type and rate of precipitation are estimated.

The POSS was mounted on a post 3 m above the field surface.

4.4 Vaisala VRG101 Precipitation Gauge

The Vaisla VRG101 uses a temperature-compensated load cell to measure the weight of precipitation collected in a container, which mounts directly at a single point on the load cell [17]. The gauge inlet funnel rests on the container, thus allowing weighing of any precipitation sticking to the funnel. The gauge has a sampling area of 400 cm^2 and a capacity of 650 mm.

At Egbert, the VRG101 gauges were installed with double alter shields.

4.5 OTT Pluvio Precipitation Gauge

There are two versions of the OTT Pluvio precipitation gauges at the Egbert test sites, Pluvio[1] and Pluvio[2] gauges. The weight of precipitation gathered in the collecting container of a Pluvio gauge is measured by a hermetically sealed electronic load cell [10] and [11]. An internal algorithm in the load cell compensates for the effect of wind and temperature variation. Due to the processing of the internal algorithm, Pluvio[1] has a delay of 9 minutes (see in [4]) in the accumulated precipitation and intensity outputs. On the other hand, Pluvio[2] has different filtering algorithms that allow for real-time (within a minute) and non-real-time (in 5 minutes) outputs. Both gauges outputs raw bucket amounts in real time. The Pluvio[1] gauges at Egbert have a collecting area of 200 cm^2 and a capacity of 1000 mm, and the Pluvio[2] gauges have a collecting area of 400 cm^2 and a capacity of 750 mm.

There are two Pluvio[1] gauges at Egbert (referred to as Pluvio[1] #1 and Pluvio[1] #2), and they were equipped with rim heating and were installed with Tretyakov style type of shields, whereas the Pluvio[2] gauges (also two units, Pluvio[2] #1 and Pluvio[2] #2) were not equipped with rim heating and were not installed with any shields.

4.6 Geonor Precipitation Gauge

Geonor T-200B gauge [1] weighs the precipitation using a load cell with a vibrating wire (VW) transducer. The Geonor gauge uses a 12-liter bucket suspended from three points, normally with 2 chains and the load cell. However, three load cells can be used with one at each point, and a Geonor gauge configured with three load cells is said to be *triple-configured*. All the Geonor gauges at the Egbert site are triple-configured. A VW transducer outputs the vibrating frequency, which is used to calculate the precipitation in depth. The Geonor gauge has a collecting area of 200 cm^2, and a capacity of 600 mm (including antifreeze liquid).

At Egbert, there are three Geonors and all were installed with alter shields, and furthermore one of Geonors was installed in the place of the manual gauge in a Double Fence Intercomparison Reference (DFIR) and served as a reference for precipitation accumulation. The DFIR is the WMO reference for solid precipitation, and it is an octagonal vertical double fence shield with a manual Tretyakov gauge at the center. See [2]. This Geonor gauge will be referred to as the Geonor in DF, and the other two as Geonor #1 and Geonor #2.

4.7 Wind Sensor

The wind sensor at 2 meter at Egbert was a RM Young 5103 anemometer, a propeller-type sensor with fuselage and tail wind vane.

4.8 Temperature and Dew Point

The temperature was measured using a Yellow Spring Inc temperature sensor. The dew point was measured using a dew cell, manufactured by Environment Canada. Both sensors were installed in a ventilated Stevenson screen.

5 Precipitation Amount Calculations

The data output by all the sensors in the test have a one-minute temporal resolution.

Both Parsivel and PWD22 output water equivalent precipitation accumulation measurements and these will be used in the comparison.

The POSS also outputs precipitation rate and accumulation measurements. However, better estimates can be obtained by post processing of the raw Doppler velocity power spectrum [12]. The new, minutely POSS precipitation rate estimates can be calculated using two different methods. The first method is called the "mass flux (MF) method". The rain drop size distribution (DSD) is estimated from the Doppler velocity spectrum. The product of the number concentration of drops, their volume, and fall velocity is summed over all the channels for different diameters to give the mass flux (rate). This method is not applicable for solid precipitation. The POSS precipitation type estimate is used to determine if the method can be applied. The second is called the "regression" method where a regression between the logarithms of 0^{th} moment of Doppler spectrum and precipitation rate is performed. This method is applicable for both liquid and solid precipitation. The precipitation accumulations are calculated by integrating the rates.

The raw bucket amounts from the weighing precipitation gauges are filtered using an algorithm developed by the Meteorological Service of Canada (MSC), and it will be referred to as the MSC-Precipitation algorithm in this paper. Roughly, it computes 5-minute averages of the raw amount every 15 minutes. If the new 5-minute average is 0.2 mm more, or 0.4 mm less than the current filtered value, the new filtered value is updated to the new 5-minute average. Otherwise, it retains the previous value. The precipitation accumulation is calculated by summing all the increases in the filtered value. The decreases are treated as evaporation loss and are not counted.

For the Geonor gauges, the MSC-Precipitation algorithm is applied to each of the three VW transducers. It turns out that, for all three gauges, the filtered accumulations of two of the three VW transducers remain close to each other, while the third diverges from the other two. The accumulation of the Geonor in DF is computed as the average of the filtered accumulations of VW transducer 1 and 3. The accumulations of Geonor #1 and #2 in alter shield are computed as the averages of filtered accumulations of VW transducer 2 and 3.

6 Precipitation and Weather during the Test Period

To give some historical perspective, the average monthly precipitation accumulations at the nearby climate station (about 3.5 km to the NW) ESSA ONT HYDRO (Latitude 44°21'N, Longitude 79°49, Elevation 216.4 m, Climate ID 6112340) are 80.4 mm (November), 80.2 mm (December), 75.6 mm (January), 51.3 mm (February), 55.7 (March), 60.4 (April), 69.4(May), and 81.9 (June). These monthly average values are based on data from 1971 to 2000.

According to the Geonor in DF, the monthly totals of precipitation are 113.2 (November), 98.6 (December), 53.0 (January), 64.2 (February), 51.7 (March), 113.9 (April), 91.7 (May), and 56 (June). According to the Geonor #1 in alter shield, the monthly totals are 91.3 (November), 79.7 (December), 39.9 (January), 58.1 (February), 51.8, (March), 104.6 (April), 92.3 (May), and 57.1 (June). The monthly totals from November 2008 to June 2009 at the OS&E Egbert test site and the climate normal are plotted in Figure 3 (a).

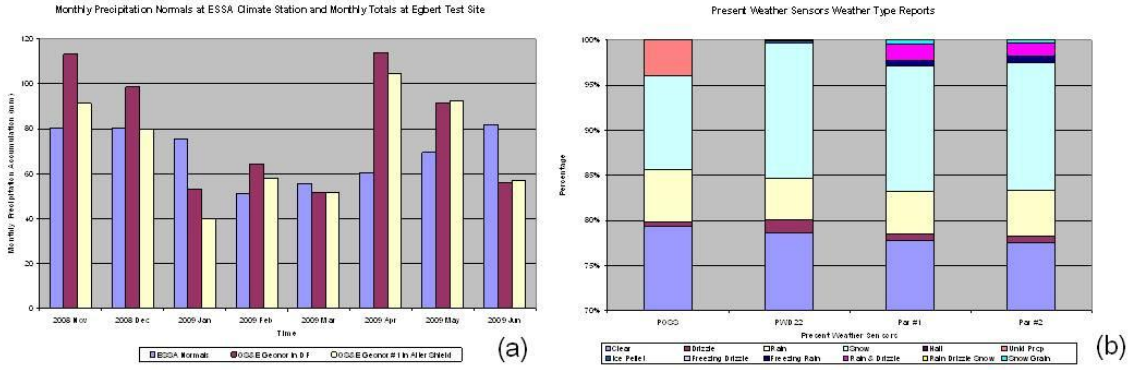

Figure 3 – (a) Monthly totals and climate normal and (b) precipitation types.

The weather reports from POSS, PWD22 and Parsivel at the test site are as follows. The dominant precipitation type during this period is snow (around 15% of the test period), and most of which is light snow. The second is rain (around 5%), and again most of which is light rain. Bar chart in Figure 3 (b) displays the relative proportions of various precipitation types. Note that the Parsivel sensor does not equip with an ambient air temperature sensor, and it can, and at times does, misidentify liquid precipitation as solid. To remedy this, the weather typing from Parsivel is modified on the basis of ambient air temperature, dew point and icing status.

7 Results

The data can be analyzed from different perspectives.

The performance of the precipitation amount measurement by the sensors can be described as the "catch ratio" of the sensor hourly estimate to the hourly reference amount. In this case the reference amount is the measurement of the Geonor in DF. The quartile statistics are used describe the distribution of these catch ratios ([14]). The median catch ratio (Q2 or 50th percentile) is an indicator of the bias. The interquartile

range (IQR) is the difference of the third (Q3 or 75th percentile) and the first (Q1 or 25th percentile) quartile, and is a measure of the dispersion of the distribution. Quartile statistics are less influenced by outliers than statistics such as mean and standard deviation [19]. A box plot is used to display the comparison, in which the lower and upper edges of the box located at Q1 and Q3, respectively, and the bar through the box at Q2. The vertical lines are drawn from the box to the most extreme point within 1.5 interquartile ranges. That is, the end of the lower line is at the minimum value that is greater than (Q1 – 1.5 IQR), and the end of the upper line is at the maximum value that is less than (Q3 + 1.5 IQR). Any data points outside this range are considered outliers and marked with crosses. The distribution is said to be positively skewed if (Q3 – Q2) > (Q2 – Q1), and is negatively skewed if (Q2 – Q1) > (Q3 – Q2).

The closeness of the data between two instruments can be described by the operational comparability (OC) – the root mean square (rms) of the difference between simultaneous readings from the two instruments measuring the same quantity in the same environment [15]:

$$OC = \sqrt{\frac{1}{N}\sum_{i=1}^{N}(X_{ai} - X_{bi})^2}$$

where N is the number of measurement, and X_{ai} and X_{bi} are the i^{th} measurements of the two instruments. If the two instruments are identical, the operational comparability is called the functional precision (FP). The means and standard deviations of the differences, and the OC, between the hourly accumulations of the sensors and the reference provide another perspective.

A paired t-test ([3]) is used to test the significance of the differences between the sensors. We will test at the 5% level of significance the hypothesis that the mean of the differences of the two sensors considered is zero.

The comparison is made only if the Geonor in DF hourly amount is greater than 0.5 mm.

The quartile statistics and outliers are presented in Figure 4 (a). It is clear that there are a number of very large outliners for the Parsivel sensors. The largest occurs for Parsivel #2, from 2:00 to 3:00 on the 16th of November, 2008. Over this hour, the Geonor in DF reported 4.62 mm of precipitation, and Parsivel #1 and #2 reported 46.27 mm and 1164.82 mm respectively. For comparison, POSS (regression) and PWD22 reported 2.70 mm and 4.33 mm respectively. The whole precipitation event started on early November 15 and continued throughout the day as rain, and then changed to snow around the start of November 16, ending around mid-day. The hourly wind started around 1.5 m/s and gradually increased to around 5 to 6 m/s at the start of November 16, peaking to 7 m/s around 4:00. It is northerly throughout the event. The temperature dropped gradually from 10°C from the beginning of the event to 0°C around 0:00 November 16, and remained around 0°C to the end of the event. Upon a closer examination of the Parsivel messages, we found that, when the precipitation accumulation of the Parsivel PWSs increases significantly above that of the others, a signal in the Parsivel output message called "signal amplitude of the laser strip" drops well below 5000, as seen in Figure 4 (b).

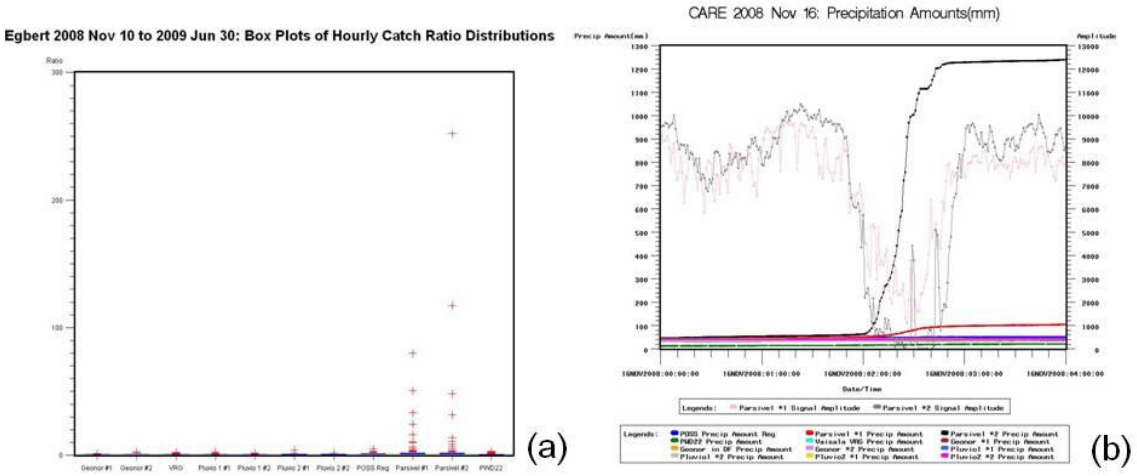

Figure 4 – (a) Catch ratios of hourly amounts, (b) Precipitation accumulations and Parsivel signal amplitudes for November 16, 2008.

This "signal amplitude" indicates the received energy of the laser, and ranges from 0 to 15000 (K. Nemeth of OTT, personal communication). The meaning of the values of this signal is as follows. From 0 to 5000, the sensor is non-operating; from 5000 to 7500, immediate maintenance or cleaning is required; from 7500 to 10000, maintenance should be in the next 3 months; and from 10000 to 15000, the sensor is operating normally.

One speculation of the cause of this significant overestimation and its apparent connection to signal amplitude is that snow accumulates on the window of the receiver and/or transmitter, thus affecting the strength of laser. The axis of the transmitter and receiver is oriented to be perpendicular to the prevailing wind which is westerly, as recommended by the operation manual [9], with the receiver facing north. The wind is northerly as noted above. It seems possible that snow was blown on to the window of the receiver. Even though there is heating, if there is sufficient snow, there might still be some snow, water or a mixture of both left on the window. As the snow lessened, the snow or water on the window gradually evaporated and the signal amplitude recovered back to the normal region.

For the rest of the analysis, the data are excluded if the signal amplitude of either Parsivel sensor drops below 7500.

The quartile statistics and outliers of the updated data set, excluding data with Parsivel signal amplitude below 7500 as described above, are presented in Figure 5 and Table 1.

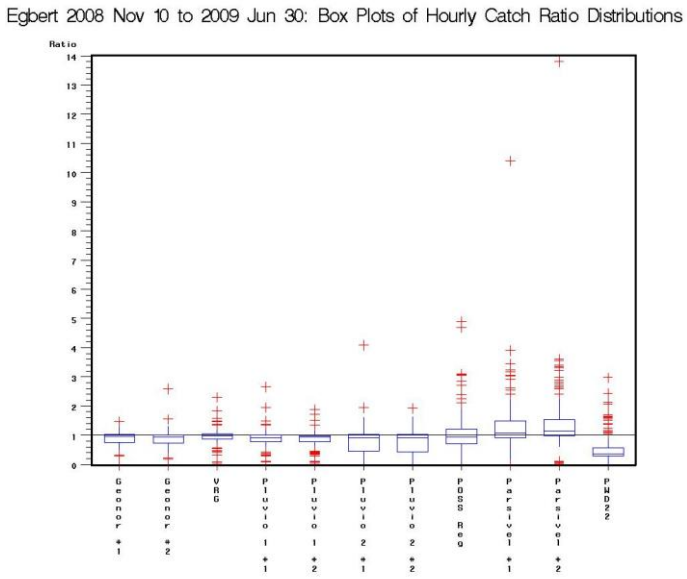

Figure 5 - Catch ratios of hourly amounts for the filtered data set.

Quartile Statistics of the Hourly Catch Ratio Distributions				
	Q1	**Q2**	**Q3**	**IQR**
POSS_Reg	0.70	0.93	1.22	0.52
Par #1	0.91	1.07	1.49	0.58
Par #2	0.98	1.14	1.54	0.56
PWD22	0.28	0.37	0.56	0.28
VRG	0.86	0.97	1.05	0.19
GNR #1	0.75	0.97	1.02	0.27
GNR #2	0.72	0.94	1.00	0.28
Plv1 #1	0.78	0.92	1.00	0.22
Plv1 #2	0.77	0.93	0.99	0.22
Plv2 #1	0.44	0.92	1.02	0.58
Plv2 #2	0.43	0.91	1.02	0.59
Number of observation: 214				

Table 1 - The quartile statistics of the catch ratio distributions.

The median of the catch ratio distribution for PWD22 is low, around 40%. It is not known what the cause is. The status and error code of the sensor indicated no problems.

The medians of both Parsivel sensors are about 110%, and the Parsivel sensors are the only sensors with medians above 100%.

The IQR, a measure of dispersion, ranges from 50% to 60% for the POSS, Parsivel sensors and Pluvio^{2} gauges. The IQR for the VRG, Geonor and Pluvio^{1} gauges is around 20% to 30%. Note that the present weather sensors and Pluvio^{2} gauges are not shielded.

The means and standard deviations of the differences, and the operational comparability, between the hourly accumulations of the sensors and the Geonor in DF are presented in Table 2.

The mean and standard deviation, and operational comparability, with respect to Geonor in DF			
Unit: mm	**mean**	**stdev**	**OC/FP**
POSS_Reg – GNR DF	0.00	1.31	1.30
Par #1 – GNR DF	0.20	1.06	1.07
Par #2 – GNR DF	0.32	1.15	1.19
PWD22 – GNR DF	-0.84	0.99	1.30
VRG – GNR DF	-0.09	0.59	0.60
GNR #1 – GNR DF	-0.14	0.42	0.44
GNR #2 – GNR DF	-0.16	0.61	0.63
Plv1 #1 – GNR DF	-0.18	0.56	0.59
Plv1 #2 – GNR DF	-0.19	0.58	0.61
Plv2 #1 – GNR DF	-0.28	0.70	0.75
Plv2 #2 – GNR DF	-0.27	0.67	0.72
Par #1 – Par #2	-0.13	0.34	0.36
GNR #1 – GNR #2	0.02	0.45	0.45
Plv1 #1 – Plv1 #2	0.01	0.24	0.24
Plv2 #1 – Plv2 #2	-0.01	0.33	0.33

Table 2 – The means, standard deviations and operational comparability.

The operational comparability of the present weather sensors is, on average, almost twice that of the gauges. The PWD22 has the largest bias and OC.

Now consider the statistics for data with mostly liquid precipitation and for data with mostly solid precipitation. The data set is first stratified into liquid and solid precipitation sets according to the present weather sensor. The precipitation types are grouped into liquid and solid precipitation as follows. Liquid Precipitation: Drizzle (L) and Rain (R) for POSS; Drizzle (L), Rain (R), Freezing Drizzle (ZL) and Freezing Rain (ZR) for PWD22; Drizzle (L), Rain (R), Rain and Drizzle (RL), and Freezing Rain (SP) for Parsivel. Solid Precipitation: Snow (S) and Hail (A) for POSS; Snow (S) and Ice Pellet (IP) for PWD22; and Snow (S), Hail (A) and Snow Grain (SG) for Parsivel. If the count of the minutely liquid precipitation reports in the hour is no less than 90% of the total identified precipitation reports of the hour, then the precipitation of the hour is considered as liquid. If the count of the minutely solid precipitation reports in the hour is no less than 90% of the total identified precipitation reports of the hour, then the precipitation of the hour is considered as solid. Otherwise, the precipitation of the hour is considered as mixed.

7.1 Liquid Precipitation

The quartile statistics and outliers for liquid precipitation are given in Figure 6 and in Table 3. Note that for liquid precipitation POSS estimates precipitation accumulation using two methods, regression and mass-flux.

It is worth noting that the medians of the catch ratio distributions of the precipitation gauges other than Pluvio[1] are within +/- 1% of the reference, and that that of Pluvio[1] at about 5% below the reference.

The medians of the catch ratio distributions for the two POSS methods are about 10 to 20% above the reference, with the regression method at 111% and mass-flux method at 118%. The Parsivel sensors have their medians of the catch ratio distributions within about +/- 5% of the reference. The median for PWD22 is well below that of the others at 33%.

The IQR for precipitation gauges are all less than about 10%. The Parsivel IQRs are about twice of that at 20%. The POSS IQRs are much larger, at about 50%. On the other hand, the PWD22 IQR is the same as that of the precipitation gauges, at 10%.

Among the present weather sensors, the performance of Parsivel appears to be closer to that of the precipitation gauges than the others.

For POSS, the results in [14] are that the medians range between 63% to 95% and IQR from 25% to 33% for mass-flux method and 30% to 45% for regression method. It should be noted that the results in [14] are based on daily accumulations, whereas in this work the statistics are generated from hourly amounts. Also, the algorithms used in estimating the precipitation rates are more recent.

One possible reason for the overestimation by POSS is the effect of splashing of raindrops impacting the radomes, as noted in [14]. The regression method appears to be less affected by splashing than the mass flux method, and this is also observed in [14]. Splashing could also contribute to the larger IQR of POSS.

The means and standard deviations of the differences, and the operational comparability and the paired t-test, between the hourly accumulations of the sensors and the Geonor in DF for liquid precipitation are presented in Table 4. The operational comparability of POSS and PWD22 (with respect to the reference) is about 6 times of that of the precipitation gauges, and that of Parsivel is about twice. PWD22 has the largest the bias and OC. In the analysis of the significance of the differences, there does not seem to be a consistent picture when comparing the present weather sensors and the gauges.

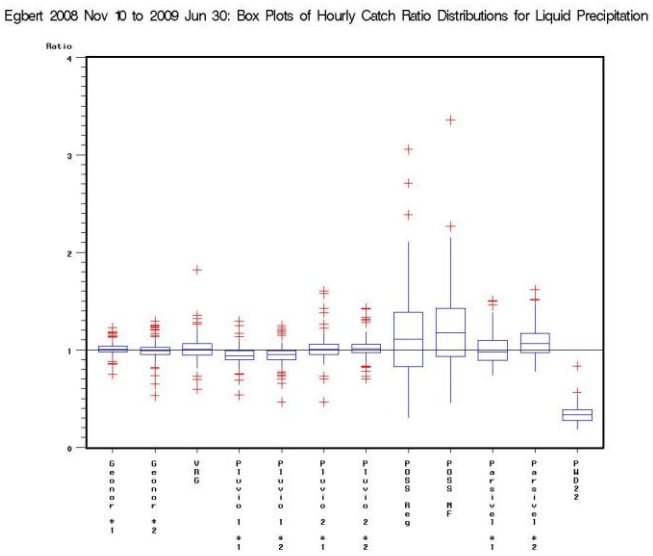

Figure 6 - Catch ratios of hourly amounts for liquid precipitation.

Quartile Statistics of the Hourly Catch Ratio Distributions for Liquid Precipitation				
	Q1	**Q2**	**Q3**	**IQR**
POSS_Reg	0.83	1.11	1.39	0.56
POSS_MF	0.93	1.18	1.43	0.50
Par #1	0.89	0.98	1.09	0.20
Par #2	0.97	1.06	1.17	0.20
PWD22	0.28	0.33	0.38	0.10
VRG	0.95	1.00	1.06	0.11
GNR #1	0.98	1.00	1.04	0.06
GNR #2	0.95	0.99	1.02	0.07
Plv1 #1	0.90	0.94	0.99	0.09
Plv1 #2	0.90	0.95	0.99	0.09
Plv2 #1	0.95	1.01	1.06	0.11
Plv2 #2	0.97	1.01	1.06	0.09
Number of observation: 110				

Table 3 - The quartile statistics of the catch ratio distributions for liquid precipitation.

The means, standard deviations, operational comparability and paired t-test with respect to Geonor in DF for liquid precipitation					
	mean (mm)	**Stdev (mm)**	**OC/FP (mm)**	**paired t-test (5% level)**	
				p-value	**mean = 0**
POSS_Reg – GNR DF	0.16	1.25	1.26	0.1723	Do not reject
POSS_MF – GNR DF	0.20	0.91	0.93	0.0226	Reject
Par #1 – GNR DF	0.00	0.28	0.28	0.9714	Do not reject
Par #2 – GNR DF	0.15	0.35	0.38	≈ 0	Reject
PWD22 – GNR DF	-1.17	0.88	1.46	≈ 0	Reject
VRG – GNR DF	0.03	0.19	0.19	0.1543	Do not reject
GNR #1 – GNR DF	0.01	0.10	0.10	0.2538	Do not reject

GNR #2 – GNR DF	-0.02	0.11	0.11	0.0761	Do not reject
Plv1 #1 – GNR DF	-0.09	0.13	0.15	≈ 0	Reject
Plv1 #2 – GNR DF	-0.08	0.14	0.16	≈ 0	Reject
Plv2 #1 – GNR DF	0.02	0.14	0.14	0.1779	Do not reject
Plv2 #2 – GNR DF	0.04	0.14	0.15	0.0114	Reject
Par #1 – Par #2	-0.15	0.21	0.26	≈ 0	Reject
GNR #1 – GNR #2	0.03	0.09	0.10	0.0012	Reject
Plv1 #1 – Plv1 #2	-0.01	0.11	0.11	0.4341	Do not reject
Plv2 #1 – Plv2 #2	-0.02	0.11	0.11	0.0735	Do not reject

Table 4 - The means, standard deviations, operational comparability and paired t-test for liquid precipitation.

The scatter plots of the hourly amounts of the present weather sensors and Geonor #1 versus the hourly amounts of the Geonor in DF for liquid precipitation are plotted in Figure 7 (a), and the scatter plots for the precipitation gauges for liquid precipitation are shown in Figure 7 (b). For these and subsequent scatter plots, the restriction, that the hourly amount of the Geonor in DF be greater than 0.5 mm, is not imposed. The intercepts, slopes and R^2 values for the regression equations are given in Table 5.

Sensors/Gauges	**Intercept**	**Slope**	**R^2 Values**
POSS Regression	0.1349	0.964	0.6777
POSS Mass-Flux	0.1867	0.9475	0.7847
Parsivel #1	0.0303	0.9967	0.9723
Parsivel #2	0.0332	1.084	0.9716
PWD22	0.023	0.3356	0.9137
VRG101	-0.001	1.0121	0.9832
Geonor #1	0.0021	1.0004	0.9944
Geonor #2	-0.0057	0.9857	0.9926
Pluvio[1] #1	-0.0205	0.9636	0.9894
Pluvio[1] #2	-0.0219	0.967	0.9903
Pluvio[2] #1	0.0076	1.0027	0.9901
Pluvio[2] #2	-0.0048	1.025	0.9889

Table 5 – The intercepts, slopes and R^2 values of the regression equations for liquid precipitation.

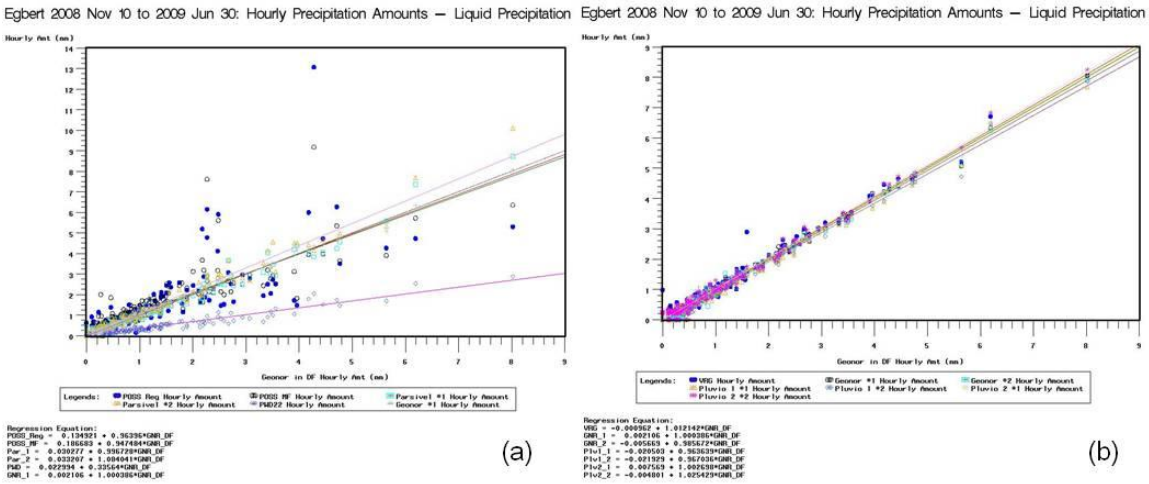

Figure 7 – (a) Scatter plots for liquid precipitation for present weather sensors, and (b) scatter plots for liquid precipitation for precipitation gauges.

7.1.1 Catch ratio vs. wind

The catch ratios for liquid precipitation are plotted against the hourly average winds for the present weather sensors in Figure 8 (a) and for the precipitation gauges in Figure 8 (b). The linear equations are fitted to the data to reflect general trends of the data.

The catch ratios of both POSS and Parsivel appear to be affected positively by the variation in wind speed, i.e., an increase in estimation with an increase in wind speed. POSS appears to be more affected than Parsivel by the variation in wind speed. The mass-flux method overestimates more than the regression method at a higher wind speed (>= 3 m/s), and at lower wind speed (< 3 m/s) there is less dispersion for the mass-flux method than for the regression method. These general characteristics of the performances of the regression and mass-flux methods are also noted in [14]. The effect of wind speed on PWD22 appears to be small. The precipitation gauges are virtually not affected by wind for liquid precipitation.

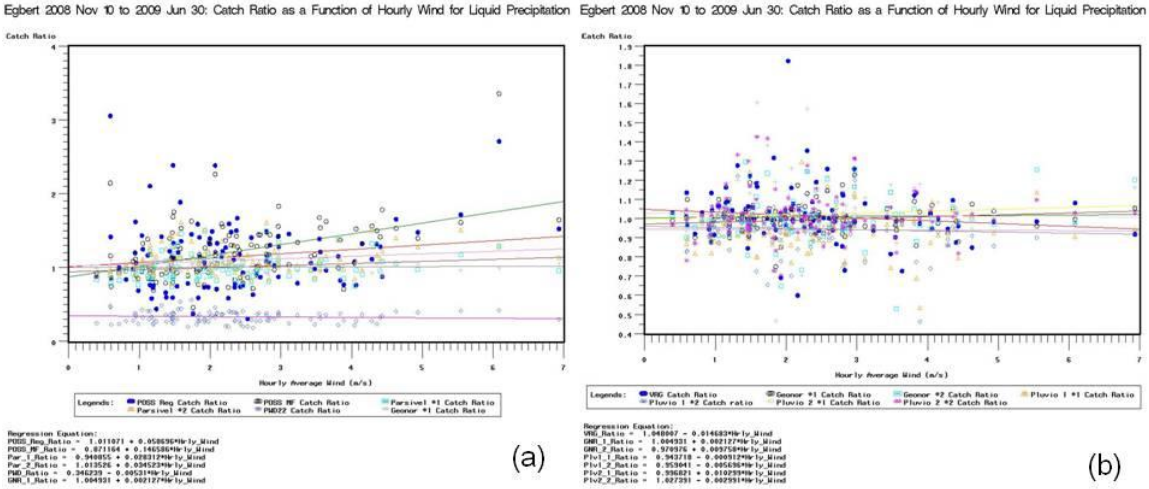

Figure 8 – (a) Catch ratios of the present weather sensors vs. hourly average winds for liquid precipitation, and (b) catch ratios of the precipitation gauges vs. hourly average winds for liquid precipitation.

7.1.2 Catch ratio vs. temperature

The catch ratios for liquid precipitation are plotted against the hourly average temperatures for the present weather sensors in Figure 9 (a) and for precipitation gauges in Figure 9 (b).

Among all the sensors and gauges, POSS appear to be the only one that is most affected by variation in temperature, with both regression and mass-flux methods varying negatively with temperature. Both methods appear to overestimate in the temperature range of 0°C to 10°C.

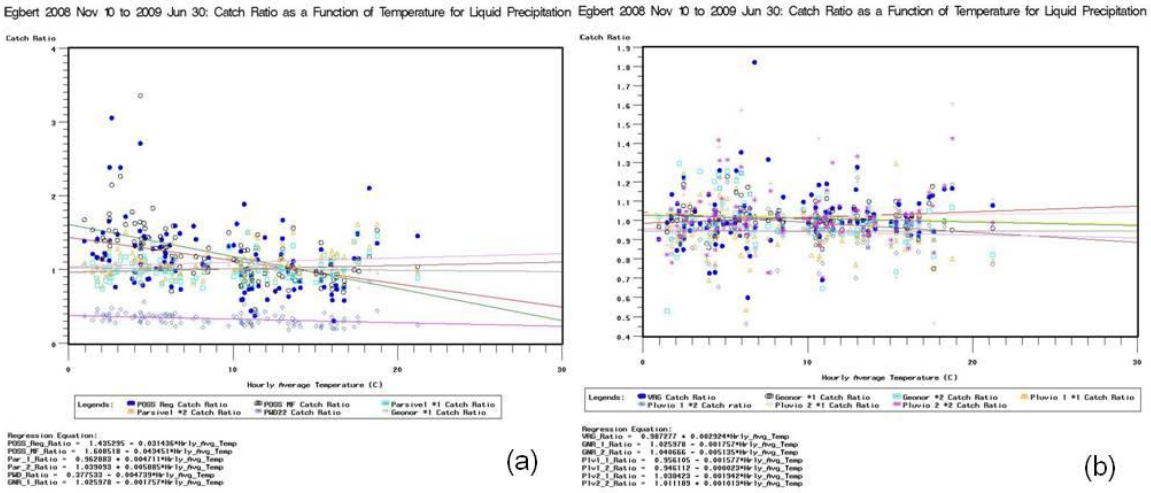

Figure 9 – (a) Catch ratios of the present weather sensors vs. hourly average temperatures for liquid precipitation, and (b) catch ratios of the precipitation gauges vs. hourly average temperatures for liquid precipitation.

7.1.3 Catch ratio vs. precipitation rate

The catch ratios for liquid precipitation are plotted against the hourly precipitation rates of the Geonor in DF for the present weather sensors in Figure 10 (a) and for precipitation gauges in Figure 10 (b).

Among all the sensors and gauges, POSS appears to be the only one that is most affected by the variation in the precipitation rate. Both the regression and mass-flux methods are affected negatively by increases in precipitation rates. The negative relationships of catch ratios vs. precipitation rates are also observed in [14].

For precipitation gauges, the dispersion of catch ratios decreases as the precipitation rate increases.

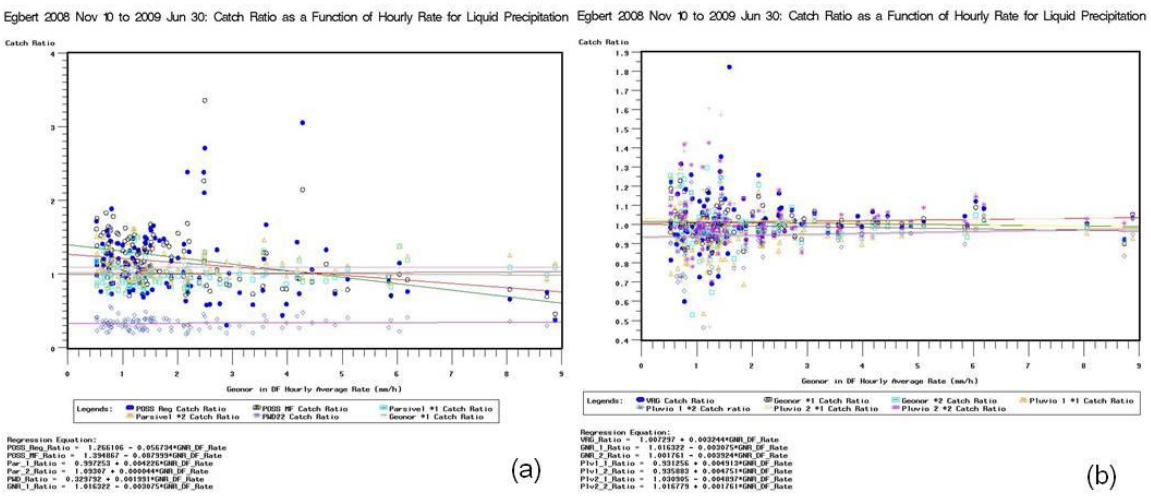

Figure 10 – (a) Catch ratios of the present weather sensors vs. hourly precipitation rates of the Geonor in DF for liquid precipitation, and (b) Catch ratios of the precipitation gauges vs. hourly precipitation rates of the Geonor in DF for liquid precipitation.

7.2 Solid Precipitation

The quartile statistics and outliers for solid precipitation are given in Figure 11 and in Table 6.

For the shielded precipitation gauges (VRG101, Geonor and Pluvio[1]), the medians of the catch ratio distributions are from 70% to 90%. For the unshielded gauges (Pluvio[2]), the medians are at about 40%.

The medians for POSS (regression) and PWD22 are 73% and 68% respectively, and they are at the lower range of the shielded precipitation gauges. On other hand, the medians of Parsivel sensors are about 50% above the reference.

The IQRs for the precipitation gauges (shielded and unshielded) are in the 30% to 40% range. For POSS, the IQR is 35%, within the range of the precipitation gauges. The IQR for PWD22 is about twice of that, at 60%, and the Parsivel IQRs are even higher, with one at 76% and the other at 93%.

Among the present weather sensors, only the performance of POSS is comparable to that of the precipitation gauges (cf. [14]). For POSS, the results in [14] are that the medians of the catch ratio distributions are from 65% to 79%, with IQR from 36% to 50%, thus comparable with the results here.

The means and standard deviations of the differences, and the operational comparability and the paired t-tests, between the hourly accumulations of the sensors and the Geonor in DF for solid precipitation are presented in Table 7 and Table 8. The operational comparability of POSS and PWD is more comparable to that of the shielded gauges than in the case for liquid precipitation, about 40% larger. The OC of Parsivel sensors is more

than twice of the shielded gauges, whereas that of the un-shielded gauges (Pluvio 2) is about 75% larger.

In the paired t-tests, all the present weather sensors and gauges are significantly different from the Geonor in Double Fence. However, when compared to the average of the shielded gauges, the differences of the POSS and PWD22 are not significant, whereas the differences of the Pasivel sensors and un-shielded gauges are significant.

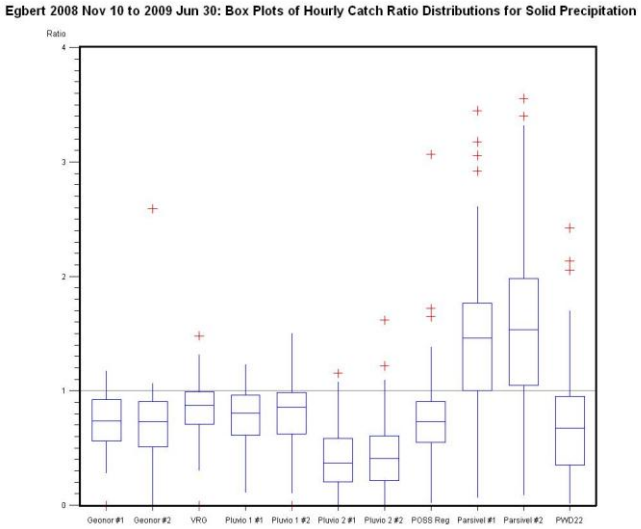

Figure 11 - Catch ratios of hourly amounts for solid precipitation.

Quartile Statistics of the Hourly Catch Ratio Distributions for Solid Precipitation				
	Q1	**Q2**	**Q3**	**IQR**
POSS_Reg	0.55	0.73	0.90	0.35
Par #1	1.00	1.46	1.76	0.76
Par #2	1.05	1.54	1.98	0.93
PWD22	0.35	0.68	0.95	0.60
VRG	0.71	0.87	0.99	0.28
GNR #1	0.56	0.73	0.92	0.36
GNR #2	0.51	0.73	0.90	0.39
Plv1 #1	0.61	0.80	0.96	0.35
Plv1 #2	0.62	0.86	0.99	0.37
Plv2 #1	0.20	0.37	0.58	0.38
Plv2 #2	0.21	0.41	0.61	0.40
Number of observation: 78				

Table 6 - The quartile statistics of the catch ratio distributions for solid precipitation.

The means, standard deviations, and operational comparability with respect to Geonor in DF for solid precipitation			
	mean (mm)	**stdev (mm)**	**OC/FP (mm)**
POSS_Reg – GNR DF	-0.26	0.54	0.59
Par #1 – GNR DF	0.44	0.87	0.97

Par #2 – GNR DF	0.53	0.82	0.97
PWD22 – GNR DF	-0.26	0.53	0.59
VRG – GNR DF	-0.18	0.33	0.38
GNR #1 – GNR DF	-0.25	0.22	0.33
GNR #2 – GNR DF	-0.22	0.56	0.60
Plv1 #1 – GNR DF	-0.21	0.35	0.41
Plv1 #2 – GNR DF	-0.19	0.34	0.39
Plv2 #1 – GNR DF	-0.58	0.46	0.74
Plv2 #2 – GNR DF	-0.53	0.51	0.74
Par #1 – Par #2	-0.09	0.37	0.38
GNR #1 – GNR #2	-0.02	0.63	0.62
Plv1 #1 – Plv1 #2	-0.02	0.19	0.19
Plv2 #1 – Plv2 #2	-0.04	0.38	0.38

Table 7 - The means, standard deviations, and operational comparability for solid precipitation.

Paired t-tests for solid precipitation **Note: Gge_avg is the average of the hourly amounts of the gauges with shields (i.e., VRG GNR #1, GNR #2, Plv1 #1, and Plv1 #2).**				
	Compared to GNR_DF		**Compared to Gge_avg**	
	paired t-test (5% level)		**paired t-test (5% level)**	
	p-value	**mean = 0**	**p-value**	**mean = 0**
POSS_Reg	≈ 0	Reject	0.3680	Do not reject
Par #1	≈ 0	Reject	≈ 0	Reject
Par #2	≈ 0	Reject	≈ 0	Reject
PWD22	≈ 0	Reject	0.3996	Do not reject
VRG	≈ 0	Reject	0.2931	Do not reject
GNR #1	≈ 0	Reject	0.2324	Do not reject
GNR #2	0.0007	Reject	0.7827	Do not reject
Plv1 #1	≈ 0	Reject	0.9266	Do not reject
Plv1 #2	≈ 0	Reject	0.2149	Do not reject
Plv2 #1	≈ 0	Reject	≈ 0	Reject
Plv2 #2	≈ 0	Reject	≈ 0	Reject
Sensors within the Same Model				
Par #1, Par #2	0.0365	Reject		
GNR #1, GNR #2	0.7532	Do not reject		
Plv1 #1, Plv1 #2	0.3705	Dot not reject		
Plv2 #1, Plv2 #2	0.3023	Do not reject		

Table 8 – Paired t-tests for solid precipitation.

The scatter plots of the hourly amounts of the present weather sensors and Geonor #1 versus the hourly amounts of the Geonor in DF for solid precipitation are plotted in Figure 12 (a), and the scatter plots for the precipitation gauges for solid precipitation are shown in Figure 12 (b). The intercepts, slopes and R^2 values for the regression equations are given in Table 9.

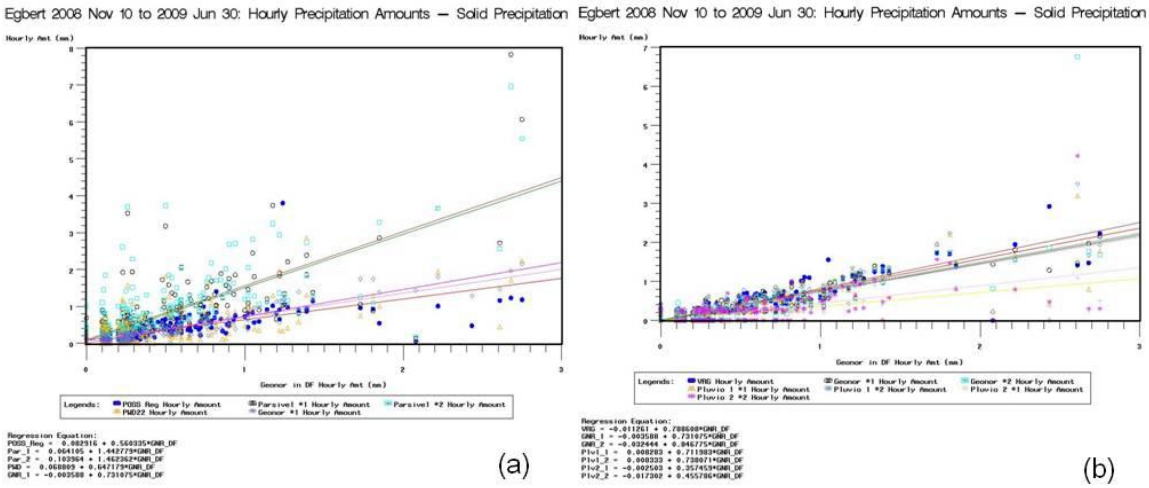

Figure 12 – (a) Scatter plots for solid precipitation for present weather sensors, and (b) scatter plots for solid precipitation for precipitation gauges.

Sensors/Gauges	Intercept	Slope	R^2 Values
POSS Regression	0.0829	0.5603	0.5724
Parsivel #1	0.0641	1.4428	0.6583
Parsivel #2	0.104	1.4624	0.6309
PWD22	0.0688	0.6472	0.5029
VRG101	-0.0113	0.7886	0.8229
Geonor #1	-0.0036	0.7311	0.8829
Geonor #2	-0.0324	0.8468	0.6706
Pluvio[1] #1	0.0083	0.712	0.7384
Pluvio[1] #2	0.0083	0.7381	0.7218
Pluvio[2] #1	-0.0025	0.3575	0.5304
Pluvio[2] #2	-0.0173	0.4558	0.4648

Table 9 - The intercepts, slopes and R^2 values of the regression equations for solid precipitation.

As it will be seen below, the overestimation of Parsivel for solid precipitation appears to be wind related.

7.2.1 Catch ratio vs. wind

The catch ratios for solid precipitation are plotted against the hourly average winds for the present weather sensors in Figure 13 (a) and for precipitation gauges in Figure 13 (b).

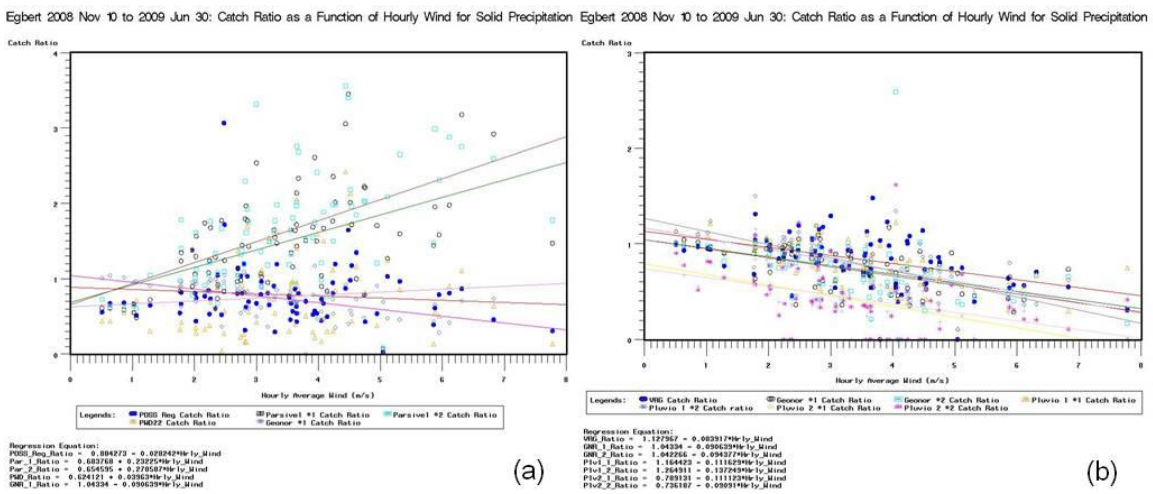

Figure 13 – (a) Catch ratios of the present weather sensors vs. hourly average winds for solid precipitation, and (b) Catch ratios of the precipitation gauges vs. hourly average winds for solid precipitation.

The catch ratios of Parsivels appear to be most, and quite strongly, affected by the increases in wind speed. The slopes of the linear regressions of both Parsivel sensors are positive, thus the catch ratio of Parsivel and wind speed correlate positively.

PWD22 also has a positive linear regression slope, but at a much smalled value. On the other hand, POSS (regression method) shows a negative, but small, slope in its linear regression. In [14], the regression method for solid precipitation shows no correlation with wind speed.

Note that at wind speeds less than 1 m/s the catch ratios of all the present weather sensors agree reasonably well with each other. As the wind speed increases, the catch ratios of Parsivel on average increase by about 25% for an increase of 1 m/s. All the present weather sensors show wider dispersions in the catch ratios as the wind speed increases with Parsivel showing the largest.

In [8] the wind induced error of rain drop size distribution measurement when using a two-dimensional video disdrometer is investigated using numerical simulation methods of computational fluid dynamics. The two-dimensional video disdrometer consists of two cameras enclosed in a large box. It is found that there is a large influence of the flow field deformation around the disdrometer body on the raindrop trajectories. Computations indicate that the error can be negative or positive, and for very small drops the error can be as high as 100%. Under certain conditions, drops can get caught in a vortex developed over the inlet and some of them might end up being measured more than once.

One can speculate that deformation to the flow fields around Parsivel and PWD22 can have similar effects on the trajectories of snow flakes, causing measurement errors. It is worth noting that the influence of wind on liquid precipitation is more limited than on solid precipitation, as the trajectories of snowflakes are more susceptible to the influence of wind.

It is interesting to note that Thies Clima recently introduced a wind shield for its Laser Precipitation Monitor (LPM) [16], whose performance on measuring precipitation rates have been studied in [5], as described earlier. It will be interesting to investigate how effective the wind shield is in reducing the influence of wind.

On the other hand, the regression method of POSS is relatively unaffected by horizontal wind [14].

The catch rations of all the precipitation gauges vary negatively with the increases in wind speed, that is, the under-catch increases as the wind speed increases, a well known fact [2].

7.2.2 Catch ratio vs. temperature

The catch ratios for solid precipitation are plotted against the hourly average temperatures for the present weather sensors in Figure 14 (a) and for precipitation gauges in Figure 14 (b).

Generally, the catch ratios for solid precipitation are not strongly affected by variation in temperature. The catch ratio of PWD22 appears to be most affected with decrease in catch ration in response to increase in temperature. POSS, on the other hand, shows a positive slope in its linear regression. Parsivel and all the precipitation gauges appear to be minimally affected with the variation in temperature.

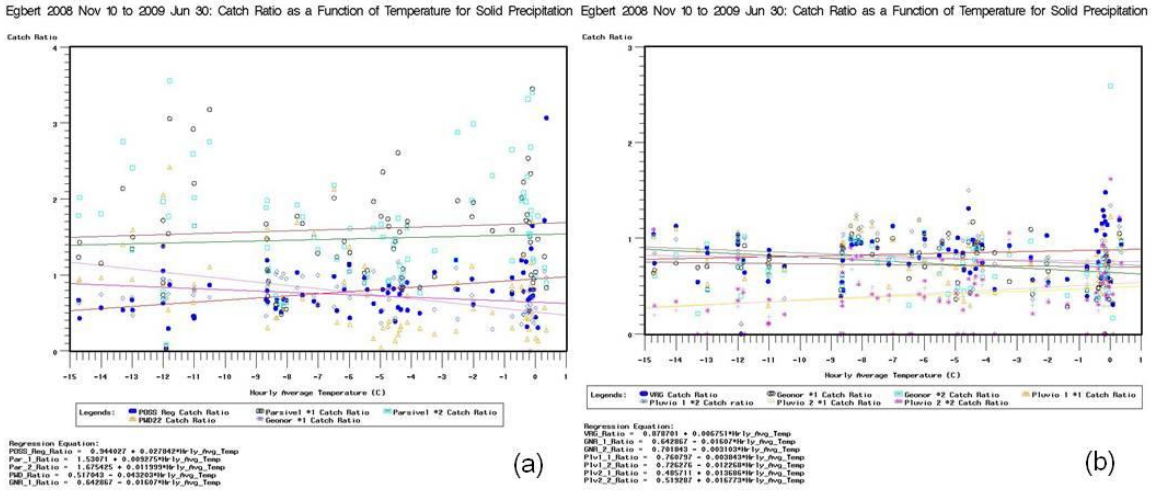

Figure 14 – (a) Catch ratios of the present weather sensors vs. hourly average temperatures for solid precipitation, and (b) catch ratios of the precipitation gauges vs. hourly average temperatures for solid precipitation.

7.2.3 Catch ratio vs. precipitation rate

The catch ratios for solid precipitation are plotted against the hourly precipitation rates of the Geonor in DF for the present weather sensors in Figure 15 (a) and for precipitation gauges in Figure 15 (b).

All present weather sensors show negative slopes in the linear regressions. Recall that POSS also shows a negative slope for liquid precipitation, but at a small (absolute) value. This behaviour of POSS in terms of catch ratios and precipitation rates for liquid and solid precipitation is also noted in [14].

The precipitation gauges do not show such consistency as the present weather sensors in their responses to the variation in precipitation rates.

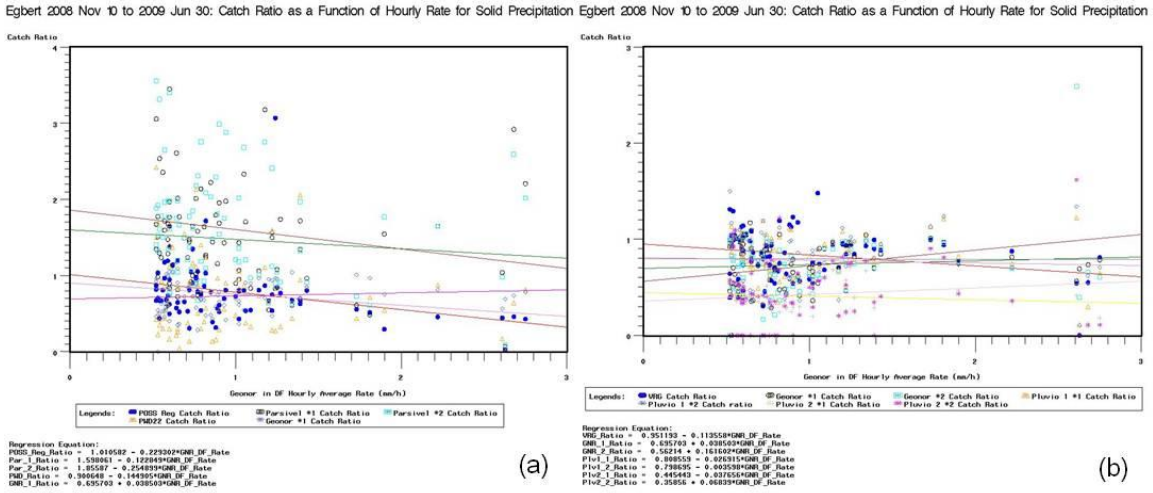

Figure 15 – (a) Catch ratios of the present weather sensors vs. hourly precipitation rates of the Geonor in DF for solid precipitation, and (b) catch ratios of the precipitation gauges vs. hourly precipitation rates of the Geonor in DF for solid precipitation.

8 Conclusions

The results are based on data with low Parsivel signal amplitude (i.e., less than 7500) excluded.

Overall, POSS is comparable to the precipitation gauges in terms of median of the catch ratio distribution, with POSS at 93% (regression method) and the (shielded) gauges ranging from 92% to 97%. However, the IQR of POSS is larger, ranging from -23% to +29% around the median, whereas the IQR of the (shielded) gauges generally is from -22% to +8%. (The negative skew is due to the effect of the undercatches of solid precipitation.) Parsivel overestimates by about 10% in terms of median; its IQR is between -16% and around +40% about the median. PWD22 underestimates by a large amount. The error code of the PWD22 did not indicate any problems; further investigation is needed to ascertain the cause.

For liquid precipitation, POSS overestimates by 11% and 18% for the regression and mass-flux methods respectively. The IQR is between -28% and +28% (regression), and

between -25% and +25% (mass-flux), about the medians. In comparison the IQR of the gauges is from -6% to +6%. Parsivel is within about 5% of the gauges in terms of median, but its IQR is from -9% to +11% about the median. PWD22 underestimates. Among the present weather sensors, POSS is most affected by the variation of wind speed, temperature and precipitation rates.

For solid precipitation, the median of POSS is at 73%, within the range of the shielded gauges (73% to 87%). The IQR of POSS is between -18% to +17% about the median, comparable to that of the shielded gauges. Parsivel overestimates by a large amount, about 50%. Its IQR is between approximately -50% to +40%. PWD22 is 68% in median, which is close to the shielded gauges, with an IQR between -33% to +27% about the median. Parsivel is most affected by the increase in wind speed. All the present weather sensors agree reasonably well with each other at wind speed less than 1 m/s. As wind speed increases, so are the dispersions for the present weather sensors, with that of Parsivel being largest. All present weather sensors decrease in catch ratio as the precipitation rate increases.

9 Acknowledgements

The author would like to acknowledge the engineering and software supports from Sorin Pinzariu and Julie Michaud for installing and maintaining the sensors and data-logging system. He is also indebted to Peter Rodriguez for his help in generating the POSS precipitation rates.

10 References

[1]. Geonor T-200B Series Precipitation Gauge User Manual, Rev. 10.3.

[2]. Goodison, B.E. and Louie, P.Y.T. and Yang, D.: WMO Solid Precipitation Measurement Intercomparison – Final Report, WMO/TD – No. 872, 1998.

[3]. Guttman, I. and Wilks, S.S. and Hunter, J.S., Introductory Engineering Statistics, Third Edition, John Wiley & Sons, 1982.

[4]. Lanza, L. and Leroy, M. and Alexandropoulos, C. and Stagi L. and Wauben, W.: WMO Laboratory Intercomparison of Rainfall Intensity Gauges, September 2004 to September 2005, Final Report.

[5]. Lanzinger, E., M. Theel, H. Windolph: Rainfall amount and intensity measured by the Thies laser precipitation monitor. In TECO-2006 WMO Technical Conference on Meteorological and Environmental Instruments and Methods of Observation, session 3. Geneva, Switzerland, 4-6 December 2006.

[6]. Löffler-Mang, M., J. Joss: An optical disdrometer for measuring size and velocity of hydrometeors. Journal of Atmospheric and Oceanic Technology, Vol. 17, 130-139, 2000.

[7]. Nemeth, K., M. Löffler-Mang: OTT Parsivel – Enhanced precipitation identifier for present weather, drop size distribution and radar reflectivity – OTT Messtechnik, Germany. In TECO-2006 WMO Technical Conference on

Meteorological and Environmental Instruments and Methods of Observation, session 1. Geneva, Switzerland, 4-6 December 2006.
[8]. Nespor, V., and W.F. Krajewski, and A. Kruger: Wind-induced error of raindrop size distribution measurement using a two-dimensional video disdrometer. Journal of Atmospheric and Oceanic Technology, Vol. 17, 1483-1492. November 2000.
[9]. Operating Instruction: Present Weather Sensor, Parsivel. OTT Messtechnik, Germany.
[10]. OTT Pluvio[1] Precipitation Gauge Installation and Maintenance Manual, OTT Messtechnik GmbH & Co. KG, Document number 70.010.390.B.E 01-0306.
[11]. OTT Pluvio[2] Precipitation Gauge Operating Instructions, OTT Messtechnik GmbH & Co. KG, Document number 70.020.000.B.E 02-0708.
[12]. Sheppard, B.E.: Description of the POSS post processed "PR" file. Notes.
[13]. Sheppard, B.E.: Measurement of raindrop size distributions using a small Doppler radar. Journal of Atmospheric and Oceanic Technology, Vol. 7, 255-268, 1990.
[14]. Sheppard, B.E., P. Joe: Performance of the precipitation occurrence sensor system as a precipitation gauge. Journal of Atmospheric and Oceanic Technology, Vol. 25, 196-212, 2008.
[15]. Standard practice for determining the operational comparability of meteorological measurement – November, 2000 ASTM committee D22 on sampling and analysis of atmospheres.
[16]. Thies Clima. Wind Protection Element, 5.4200.00.000, 021576/10/09, www.thiesclima.com.
[17]. User's Guide: Vaisala All Weather Precipitation Gauge VRG101, M210729EN-A, March 2006.
[18]. User's Guide: Vaisala Present Weather Detector PWD22. Vaisala 2006.
[19]. Wilks, D.S.: Statistical Methods in the Atmospheric Sciences. Second Edition. Academic Press.
[20]. Wong, K., Fischer, A., Ritu, R.: Measurement of precipitation at AWS in Canada: configuration, challenges and alternative approaches. TECO-2008.